ICAS 2021 SHANGHAI
32nd Congress of the International Council of the Aeronautical Sciences
September 6-10, 2021 Pudong Shangri-La, Shanghai, China

MEMS-BASED DISTRIBUTED NAVIGATION SYSTEM

Liu Zhao[1], Chen Pu[1], Wei Xue-dong [1]

Xi'an Flight Automatic Control Research Institute Shaanxi China [1]

Abstract

With the continuous development of on-board communication capabilities, processor computing capabilities, and data fusion technologies, it has become possible for multiple sets of inertial sensors with different accuracy to form an inertial network on board. The airborne inertial network can not only provide the overall motion measurement information of the aircraft, but also obtain high-precision measurement information of the local motion state. Using the rich redundant measurement information in the inertial reference system, the fault tolerance improvement method of the inertial reference system is studied, and different fusion methods are designed for the possible practical application scenarios of the distributed inertial reference system: forward and backward navigation fusion methods It can provide high-precision post-processing local absolute inertial measurement information; by modeling the wing's dynamics and designing the federal Kalman filter, it can monitor the deformation of the typical airframe structure (wing).

Keywords: inertial network, relative inertial navigation, MEMS sensor, information fusion method

1. Introduction

With the development of airborne high-speed data communication networks, the distributed integrated modular structure of airborne electronic equipment has been introduced into modern fighter systems. The volume and cost of the inertial measurement unit have been reduced, the fault tolerance and reliability have been improved, as well as the development of filtering technology, information fusion technology and computer technology, and the above-mentioned advanced fighters are more dependent on inertia. Information and higher reliability and accuracy requirements, these factors together contributed to the establishment, research, and development of the concept of distributed inertial sensor networks. The distributed inertial network integrates the output information of the inertial system distributed on the carrier and the inertial system that may be added. After data processing, more reliable and accurate navigation information and local motion state are obtained, so that any network node can maintain a sufficiently accurate inertial state to complete the purpose of navigation, inspection and even vehicle body structure inspection.

Aiming at the performance requirements for accurate and reliable acquisition of the inertial state of key aircraft sensor positions, this paper focuses on the analysis of the architecture of the MEMS-based distributed inertial reference system based on the theory of inertial navigation systems. A dynamic model between the master and slaver INS has been established, and certain research results have been obtained, which can provide theoretical basis and engineering value for the expansion of the inertial navigation system.

2. Relative navigation algorithm

In order to obtain the relative inertial parameters between the master and slaver INS, there is a very intuitive method to obtain the measurement information of the mINS and sINS in the navigation coordinate system separately, and then the position and velocity vector difference is calculated. Obtain the relative position and relative speed, and use the relational formula to obtain the direction cosine matrix to obtain the relative attitude angle. However, because the accuracy of the sINS is often several orders of magnitude different from that of the mINS, the inertial navigation of the sINS itself is just There is a large measurement error. Secondly, because the relative distance between the master and slaver INS is relatively short, generally on the meter level, then the output value of the relative navigation and the radius of the earth have a huge magnitude difference, and the relative measurement between the main and sub-nodes cannot be guaranteed accuracy. In

response to this problem, a method of relative navigation inertial calculation is proposed here: After the relative navigation is calculated directly using the inertial measurement information of the main and sub-nodes, it is then fused with the high-precision inertial measurement information provided by the mINS to obtain sINS absolute navigation information [1].

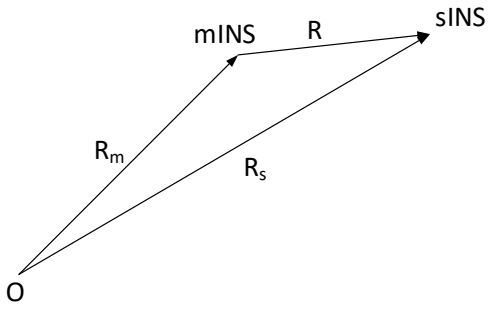

Figure 1– Schematic diagram of relative position.

The relative position diagram of the master and slaver INS is shown in Figure 1. Select the earth coordinate system as the position reference system, Then the mINS position vector is a straight line from the origin of the earth coordinate system to the origin of the main inertial navigation system, In the same way, the sINS position vector can be obtained. The position vector from the sINS to the mINS is R[2]. Obviously, when the positional relationship vector between the master and slaver INS is described by rectangular coordinate parameters, the relative position relationship is

$$\boldsymbol{R}_s = \boldsymbol{R}_m + \boldsymbol{R} \tag{1}$$

Differentiate the two sides of the relative position relationship at the same time, from the Coriolis theorem, we can get:

$$\left.\frac{d\boldsymbol{R}_s}{dt}\right|_e = \left.\frac{d\boldsymbol{R}_m}{dt}\right|_e + \left.\frac{d\boldsymbol{R}}{dt}\right|_e == \left.\frac{d\boldsymbol{R}_m}{dt}\right|_e + \left.\frac{d\boldsymbol{R}}{dt}\right|_m + \boldsymbol{\omega}_{em} \times \boldsymbol{R} \tag{2}$$

Abbreviated as:

$$\dot{\boldsymbol{R}}_s^e = \dot{\boldsymbol{R}}_m^e + \left.\frac{d\boldsymbol{R}}{dt}\right|_m + \boldsymbol{\omega}_{em} \times \boldsymbol{R} \tag{3}$$

Projecting it to the geographic coordinate system, the following relationship can be obtained:

$$\boldsymbol{V}_s^e = \boldsymbol{V}_m^e + \boldsymbol{C}_m^n \left.\frac{d\boldsymbol{R}}{dt}\right|_m + \boldsymbol{C}_m^n \left[\left(\boldsymbol{\omega}_{im}^m - \boldsymbol{\omega}_{ie}^m\right) \times \boldsymbol{R}\right] \tag{4}$$

This is the relative speed relationship between the mINS and sINS. Relative posture relationship is:

$$\boldsymbol{C}_s^m = \boldsymbol{C}_b^m \boldsymbol{C}_m^s \tag{5}$$

The above three formulas(1)(4)(5) together constitute the relative motion relationship, based on which the Relative navigation solution model can be derived, as shown below:

$$\begin{cases} \dot{\boldsymbol{C}}_s^m = \boldsymbol{C}_s^m \left(\boldsymbol{\omega}_{is}^s \times\right) - \left(\boldsymbol{\omega}_{im}^m \times\right) \boldsymbol{C}_s^m \\ \dot{\boldsymbol{V}}_{ms}^m = \boldsymbol{C}_s^m \boldsymbol{f}_{sfs}^s - \boldsymbol{f}_{sfm}^m - 2\boldsymbol{\omega}_{im}^m \times \boldsymbol{V}_{ms}^m - \dot{\boldsymbol{\omega}}_{im}^m \times \boldsymbol{R}^m - \boldsymbol{\omega}_{im}^m \times \left(\boldsymbol{\omega}_{im}^m \times \boldsymbol{R}^m\right) \\ \dot{\boldsymbol{R}}^m = \boldsymbol{V}_{ms}^m \end{cases} \tag{6}$$

3. Relative navigation error model and compensation method

The relative navigation algorithm is a differential equation derived based on the law of inertia. In the process of inertial settlement, errors will continue to accumulate, leading to divergence of the solution results, so the error compensation algorithm must be studied.

Record the real relative posture matrix as $\boldsymbol{C}_m^s$, the calculated relative posture as $\tilde{\boldsymbol{C}}_m^s$, and the conversion matrix between and as $\boldsymbol{C}_m^{m'}$, the corresponding equivalent rotation vector is ϕ, obviously

there is a relation:

$$\boldsymbol{C}_s^{m'}=\boldsymbol{C}_m^{m'}\boldsymbol{C}_s^m=\left[\boldsymbol{I}-(\boldsymbol{\phi}\times)\right]\boldsymbol{C}_s^m \tag{7}$$

The update formula of the attitude matrix including the error is:

$$\dot{\boldsymbol{C}}_s^{m'}=\boldsymbol{C}_s^{m'}\left(\tilde{\boldsymbol{\omega}}_{is}^s\times\right)-\left(\boldsymbol{\omega}_{im}^m\times\right)\boldsymbol{C}_s^{m'} \tag{8}$$

Substituting (7)into(8), after unfolding, the product of the relative attitude error and the gyro measurement (second-order small amount) is omitted, and we can get the relative attitude error equation is:

$$\dot{\boldsymbol{\phi}}=\boldsymbol{\phi}\times\boldsymbol{\omega}_{im}^m-\boldsymbol{\delta}\boldsymbol{\omega}_{is}^m \tag{9}$$

Like the process of establishing the relative attitude error equation, rewrite the relative navigation speed update differential equation containing the error as:

$$\dot{\tilde{\boldsymbol{V}}}^m=\tilde{\boldsymbol{C}}_s^m\tilde{\boldsymbol{f}}_{sfs}^s-\boldsymbol{f}_{sfm}^m-2\boldsymbol{\omega}_{im}^m\times\tilde{\boldsymbol{V}}^m-\dot{\boldsymbol{\omega}}_{im}^m\times\tilde{\boldsymbol{R}}^m-\boldsymbol{\omega}_{im}^m\times\left(\boldsymbol{\omega}_{im}^m\times\tilde{\boldsymbol{R}}^m\right) \tag{10}$$

Subtract from the second formula in formula (6), The differential equation of relative navigation speed error can be obtained:

$$\boldsymbol{\delta}\dot{\boldsymbol{V}}=\boldsymbol{C}_s^m\boldsymbol{f}_{sfs}^s\times\boldsymbol{\phi}-2\boldsymbol{\omega}_{im}^m\times\boldsymbol{\delta V}-\dot{\boldsymbol{\omega}}_{im}^m\times\boldsymbol{\delta R}-\boldsymbol{\omega}_{im}^m\times\left(\boldsymbol{\omega}_{im}^m\times\boldsymbol{\delta R}\right)+\boldsymbol{C}_s^m\boldsymbol{\delta f}_{sfs}^s \tag{11}$$

The relative position error is the integral of the relative speed error:

$$\delta\dot{\boldsymbol{R}}=\delta\boldsymbol{U}-\boldsymbol{\omega}_{im}^m\times\delta\boldsymbol{R} \tag{12}$$

Equation(9), (11), (12) together constitute a complete error model of relative inertial navigation. According to the error model, a Kalman filter can be established to compensate for the error in the relative navigation inertia settlement process

4. Information Fusion Method

Using the network structure of the distributed inertial network reference system, the constraint relationship and network structure between the sub-nodes can be used to monitor the body deformation and solve some problems that may be encountered in actual use situations[3], such as: When a certain sub-inertial navigation has a problem when the system is working, how to identify the specific problematic sub-node, etc., has become an important task of the data fusion method of the distributed inertial network reference system.

4.1 System fault tolerance improvement method

For multi-sensor systems, the introduction of fault detection and isolation technology into the system can effectively improve the fault tolerance of the navigation system, so that the system can complete the task more stably. This section will design a fault-tolerant solution for the distributed inertial reference network. Based on a networked structure, the information between multiple sub-inertial navigations will be integrated and processed, and a filter bank will be formed to provide system fault detection and isolation functions. Finally, the fault tolerance of the system is improved.

The purpose of fault detection and isolation is to detect the faults of the sub-inertial navigation on-line, isolate the sub-inertial navigation that has failed, so that the sub-inertial navigation does not participate in the work of the system, and prevent the appearance of wrong information or the pollution of the entire distributed system due to the failure of a single sub-inertial navigation The case of the baseline system appears. Sensor failures can usually be divided into hard failures and soft failures according to the degree of failure. Hard fault refers to the fault caused by the damage of the sensor hardware. Generally, the value is large and changes suddenly, which is also called complete fault. Usually when a hard fault occurs, the output value is no longer the real measured value, and will always remain a certain value. Depending on the device, it may be 0 or the upper limit of the amplitude. From the graph of the output value, it will be a horizontal line. The soft fault generally refers to the variation of sensor characteristics, with small amplitude and slow change. Soft faults generally include data deviation, accuracy degradation, etc. Soft faults change slowly and are difficult to find. In a sense, they are more harmful to the system than hard faults.

Considering that the distributed inertial reference network system has no external measurement, the sensor type is single, and the structure is more restrictive, the fault detection and isolation method adopts three levels of detection, which are divided into: subsystem output correlation detection, Kalman filter measurement Residual error detection, reasonableness detection of filter state. The detection process is shown in Figure 5.1:

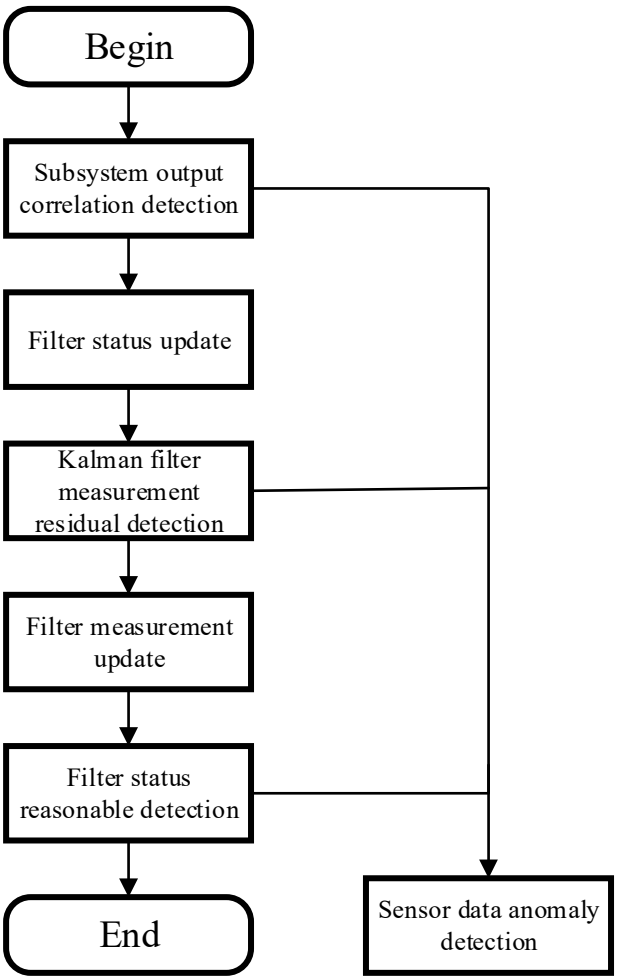

Figure 2-Fault detection flow chart

4.1.1 Subsystem output correlation detection

For distributed inertial systems, the overall system is arranged in different parts of the aircraft, and the output values of each sub-node show strong correlation[4]. These correlations are also reflected in the redundancy of measurement information and provide conditions for fault detection. Under normal conditions, the difference between the measured values of each sub-inertial navigation should be within a certain range. If a certain sub-inertial navigation fails, its output value will inevitably have a large gap with other sub-inertial navigation. The difference between the output of the two sub-inertial navigation and the specified threshold can be used to determine the faulty subsystem. Each sub-sensor can output the three-axis speed and angular velocity increment of its own reference coordinate system, and use these quantities to perform fault detection and determine the faulty subsystem.

Suppose there are 3 sub-inertial navigations arranged in the system, which are called sINS1, 2, 3. Take the x-axis accelerometer output f_{sfx} of three sub-inertial navigation as an example, T is the fault detection threshold.

Comparison between sINS1 and sINS2 (I): $\left|f_{sfx1}-f_{sfx2}\right|>T$

Comparison between sINS1 and sINS3 (II): $\left|f_{sfx1}-f_{sfx3}\right|>T$

Comparison between sINS2 and sINS3 (III): $\left|f_{sfx2}-f_{sfx3}\right|>T$

If the above fault conditions are met, the corresponding flag position is set to 1, otherwise the flag is recorded as 0. It can also be clearly seen from the above fault conditions that if there is a problem with sub-inertia 1, then the judgment conditions 1 and 2 will both meet the fault conditions. This also allows us to use the flag bit according to the voting mechanism to uniquely determine the faulty sINS.

4.1.2 Kalman filter measurement residual detection

The discrete system model with fault is:

$$\begin{cases} \boldsymbol{X}(k) = \boldsymbol{F}(k,k-1)\boldsymbol{X}(k-1) + \boldsymbol{W}(k-1) \\ \boldsymbol{Z}(k) = \boldsymbol{H}(k)\boldsymbol{X}(k) + \boldsymbol{V}(k) + \boldsymbol{\rho}(k,\theta) \end{cases} \tag{13}$$

Among them, $\boldsymbol{\rho}(k,\theta)$ is the failure function, θ is the time when the failure occurs, and the rest of the symbol definitions are the same as before. When there is no fault, the measurement residual of the Kalman filter is:

$$\boldsymbol{\gamma}(k) = \boldsymbol{Z}(k) - \boldsymbol{H}(k)\boldsymbol{F}(k,k-1)\hat{\boldsymbol{X}}(k) \tag{14}$$

At this time, the residual should be Gaussian white noise with zero mean, and its modified covariance is:

$$\boldsymbol{A}(k) = \boldsymbol{H}(k)\boldsymbol{P}(k,k-1)\boldsymbol{H}^{T}(k) + \boldsymbol{R}(k) \tag{15}$$

Construct a fault detection function:

$$\boldsymbol{\lambda}(k) = \boldsymbol{\gamma}^{T}(k)\boldsymbol{A}^{-1}(k)\boldsymbol{\gamma}(k) \tag{16}$$

Since $\boldsymbol{\gamma}(k)$ is a Gaussian random vector, $\boldsymbol{\lambda}(k)$ should obey the χ^2 distribution with m degrees of freedom, that is, the fault judgment condition is:

$$\begin{cases} \boldsymbol{\lambda}(k) > \sigma & \text{fault} \\ \boldsymbol{\lambda}(k) \le \sigma & \text{no-fault} \end{cases} \tag{17}$$

σ is the preset threshold, which can be known from the Newman-Pearson criterion, and the threshold can be obtained from the false alarm rate $P_{fa} = P\left[\lambda(k) > \sigma\right] = \alpha$. When the residual error of a certain filter is detected and reported, it is determined that the corresponding sINS is faulty.

4.1.3 Filter status reasonable detection

The two rounds of detection described above are mainly for hard fault detection, and the rationality detection of the filter state is for soft fault detection. Also suppose that there are 3 sINS, namely sINS1,2,3, corresponding to 3 filters, namely F1, F2, F3. Design the shadow filters F1_s, F2_s, F3_s corresponding to the three filters. The shadow filter does not update the measurement, only time update, and use the state of F1, F2, F3, and the variance matrix to reset F1_s, F2_s, F3_s every 300s. Build state residuals:

$$\boldsymbol{\beta}_k = \boldsymbol{X}_k^{s}(7,8,9) - \boldsymbol{X}_k(7,8,9) \tag{18}$$

Then construct the residual matrix of the covariance matrix:

$$\boldsymbol{T}_k = \boldsymbol{P}_k^{s}(7:9,7:9) - \boldsymbol{X}_k(7:9,7:9) \tag{19}$$

When the determinant of the residual matrix of the covariance matrix is not zero, that is $|T_k| \neq 0$, and the condition number of T_k is less than 100, the fault detection statistics are calculated:

$$\lambda_K = \beta_K^{\mathrm{T}} T_K^{-1} \beta_K \tag{20}$$

If λ_K >23, it is determined that the corresponding filter works abnormally, that is, the state of the sub-inertial navigation corresponding to the filter is abnormal, and no-fault detection is performed when the conditions are not met.

The above is the whole content of the distributed inertial network fault detection mechanism.

4.2 Information Fusion Method of Distributed Inertial Reference System

As we all know, the wing is the main structure that provides lift for the aircraft. During the flight of the aircraft, due to the influence of various complicated airflows on the fuselage, the wing will be elastically deformed. Although a lot of simulation analysis and calculation analysis are carried out in the process of aircraft design and manufacturing, in actual flight conditions, the airflow and the wing deformation are coupled together, which makes the wing deformation very complicated. Although the strength and durability of the wing will be guaranteed through design, in the actual flight process, the wing will be heavily loaded during each flight. The overload perpendicular to the wing plane will cause the wing to bear the greatest dynamic structural load. Generally, the wing tip of a large aircraft with a wingspan of 40-50m fluctuates more than one meter during flight. Such a huge load will cause fatigue damage to the wings and reduce the safety of the aircraft[5]. The fatigue damage is difficult to judge from the

appearance, and since there is no real data on the deformation of the wing in the air, it is impossible to analyze the damage of the parts and the deformation of the wing. Therefore, the inspection of the wing during flight is very important. Necessary.
This section will establish a specific method of using distributed inertial sensor network for wing deformation detection, mainly to monitor the longitudinal deformation of the wing.

4.2.1 Modeling of wing flexural deformation

The schematic diagram of the deformation of the wing is shown:

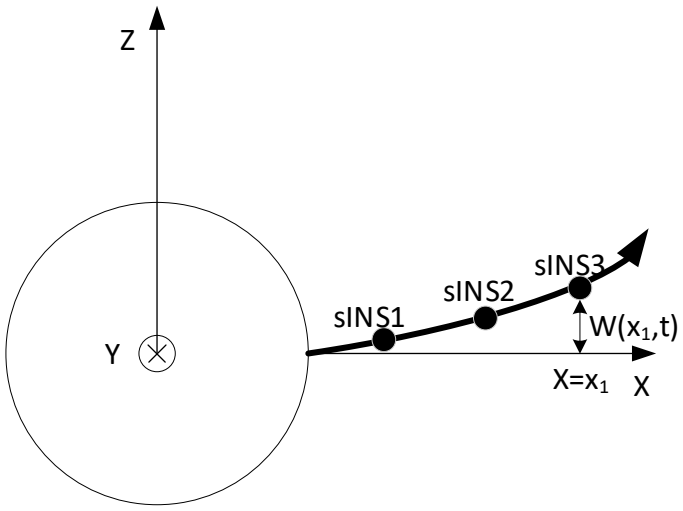

Figure 3-Schematic diagram of wing deformation

The deformation of the wing is modeled by the theory of thin plate bending. The form of the basic mechanical equation of thin plate bending is as follows:

$$\frac{\partial^4 w}{\partial x^4}+2\frac{\partial^4 w}{\partial x^4 y^2}+\frac{\partial^4 w}{\partial y^4}=\frac{q(x,y)}{D} \tag{21}$$

In the equation (21), *w* is the deflection, which refers to the displacement of the midplane of the thin plate perpendicular to the midplane under the action of the load q. , *x, y* are the coordinate points along the *x* and *y* axes of the thin plate, *q(x, y)* is the load of the treatment and the middle of the thin plate, and *D* is the bending stiffness of the thin plate. From the formula, we can see that when the boundary conditions are determined, the deflection w can be determined by the load. Considering only the deflection produced along the direction perpendicular to the plane of the wing, the partial derivatives of w with respect to *y* are 0, so equation(21) can be simplified as:

$$\frac{\partial^4 w}{\partial x^4}=\frac{q(x,y)}{D} \tag{22}$$

Assuming that the bending moment and transverse shear force at the end of the wing are 0, when $x=L_w$, there is:

$$\begin{cases} M_x=0\Rightarrow\dfrac{\partial^2 w}{\partial x^2}=0 \\ Q_x=0\Rightarrow\dfrac{\partial^3 w}{\partial x^3}=0 \end{cases} \tag{23}$$

One end of the wing is fixed to the fuselage without deformation, Based on the above, the deflection deformation model of the wing can be obtained by integration:

$$w=\frac{q}{24D}\left(x^4-4L_w x^3+6L_w^2 x^2\right) \tag{24}$$

However, in the actual flight process, the load *q* and the bending stiffness *D* are not known to us. The deflection deformation at the end of the wing can be obtained by doing the deformation $q=8w_L D/L_w^4$. The deflection is re-expressed as:

$$w = \frac{w_L}{3L_w^4}\left(x^4 - 4L_w x^3 + 6L_w^2 x^2\right) \tag{25}$$

From the above formula, we can see that the length of the wing is known, when the deflection deformation of the wing tip is determined, the deflection at any position of the wing can be determined, and the deflection of the wing tip corresponds to the only kind of wing deformation; Conversely, when the deflection and position of a certain position of the wing are known, the deflection of the end of the wing can also be determined. That is to say, after the sub-inertial navigation is arranged on the wing, the position of each sub-inertial navigation and the measured deflection can be used to determine a kind of wing deformation.

4.2.2 Federated Kalman Filter Algorithm

Considering that the shape estimation of the wing requires the comprehensive utilization of the solution results of multiple sub-nodes[6], the federated Kalman filter structure will be used for fusion. The structure of the federated Kalman filter is shown in the figure below:

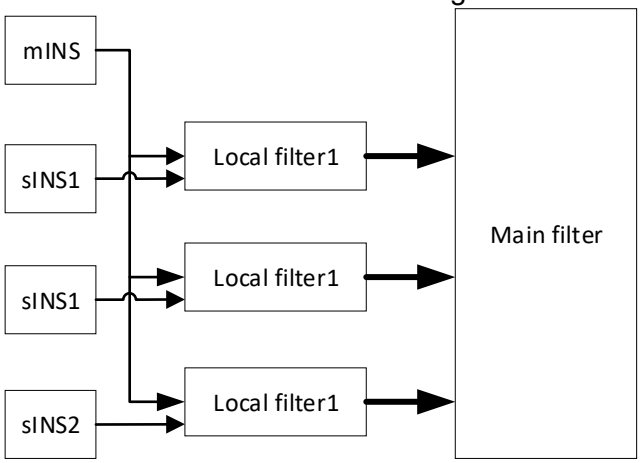

Figure 4-Schematic diagram of federated filter structure

In the federated Kalman filter, the system information update can be divided into 4 parts:

1) Information distribution

In the federated Kalman filter, the system has a common state, and the common state is filtered in the main and sub-filters. The main filter is responsible for the distribution of the covariance matrix *P* and the noise variance matrix of the common state in the sub-filter according to the variance upper bound technique:

$$\begin{aligned} \boldsymbol{P}_{i,0} &= \boldsymbol{\beta}_i^{-1}\boldsymbol{P}_0 \\ \boldsymbol{Q}_{i,0} &= \boldsymbol{\beta}_i^{-1}\boldsymbol{Q}_0 \end{aligned} \tag{26}$$

In equation (26), $\boldsymbol{P}_{i,0}$ is the covariance matrix corresponding to the common state in the i-th sub-filter, $\boldsymbol{Q}_{i,0}$ is the noise variance matrix corresponding to the common state in the i-th sub-filter, and β_i is the information distribution factor, which can be determined by the designer according to the specific The situation is set, but the law of conservation of information[7] must be satisfied:

$$\sum_i^n \beta_i = 1 \tag{27}$$

2) Time update

In each sub-filter, the time is updated according to the Kalman filter:

$$\begin{aligned} \boldsymbol{X}_{i,K/K-1} &= \boldsymbol{\Phi}_{i,K/K-1} \cdot \boldsymbol{X}_{i,K-1} \\ \boldsymbol{P}_{i,K/K\text{-}1} &= \boldsymbol{\Phi}_{i,K/K\text{-}1} \times \boldsymbol{P}_{K\text{-}1} \times \boldsymbol{\Phi}_{i,K/K\text{-}1}^T + \boldsymbol{Q}_{i,K\text{-}1} \end{aligned} \tag{28}$$

3) Measurement update

The measurement of the sub-filter is updated to:

$$\begin{aligned} \boldsymbol{K}_K &= \boldsymbol{P}_{K|K-1} \cdot \boldsymbol{H}_K^{\mathrm{T}} \cdot (\boldsymbol{H}_K \cdot \boldsymbol{P}_{K|K-1} \cdot \boldsymbol{H}_K^{\mathrm{T}} + \boldsymbol{R}_K)^{-1} \\ \boldsymbol{X}_K &= \boldsymbol{X}_{K|K-1} + \boldsymbol{K}_K \cdot \boldsymbol{Z}_K \\ \boldsymbol{P}_K &= (\boldsymbol{I} - \boldsymbol{K}_K \cdot \boldsymbol{H}_K)\boldsymbol{P}_{K/K-1}(\boldsymbol{I} - \boldsymbol{K}_K \cdot \boldsymbol{H}_K)^T + \boldsymbol{K}_K \boldsymbol{R}_K \boldsymbol{K}_K^T \end{aligned} \tag{29}$$

4) Information fusion

Information fusion is performed after the main filter obtains the state covariance matrix and state vector of all sub-filters:

$$\begin{aligned} \boldsymbol{P}_k &= \left(\sum_{i=1}^{n} P_{i,k}^{-1} \right)^{-1} \\ \boldsymbol{X}_k &= P_k \sum_{i=1}^{n} P_{i,k}^{-1} X_{i,k} \end{aligned} \tag{30}$$

Select the deflection displacement of the wing tip X_{bi}^T as the common state. Rewrite the state vector, and rewrite the state variable in the i-th sub-filter as:

$$\boldsymbol{X}_i = \left[\boldsymbol{X}_{ci}^T, \boldsymbol{X}_{bi}^T \right]^T \tag{31}$$

The fusion method of the main filter is:

$$\begin{aligned} \boldsymbol{P}_k &= \left(\sum_{i=1}^{n} P_{i,k}^{-1} \right)^{-1} \\ \boldsymbol{X}_k &= P_k \sum_{i=1}^{n} P_{i,k}^{-1} X_{i,k} \end{aligned} \tag{32}$$

5. Experiments and simulation results

5.1 Relative navigation error model and compensation method

The flight trajectory is set as: the carrier starts from the same position with a heading angle of 30°, passes through two S-shaped turns, and then conducts regular maneuvers such as level flight, turn, level flight at a constant speed, and the duration is 10 minutes, sampling time is 2.5ms.

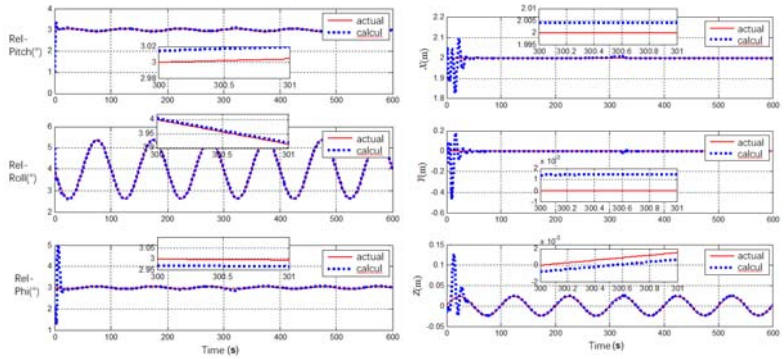

Figure 5 - Relative attitude and relative position

The average relative attitude error is [0.10', -0.04', 0.93'], and the average relative position error is [0.38mm, -0.33mm, 0.84mm].

5.2 Information Fusion Method of Distributed Inertial Reference System

Assuming that five sINS are distributed on the right side of the wing, the specific setting conditions are shown in Table 1.

Table 1 - sINS setting parameter table

sINS Number	Distance to main node (m)	Deformation amplitude (mm)	Gyro drift (°/h)	Accelerometer Bias(ug)
1	1	7	0.1	20
2	2	23	0.5	100
3	3	48	0.1	20
4	4	74	0.1	100
5	5	100	0.1	20

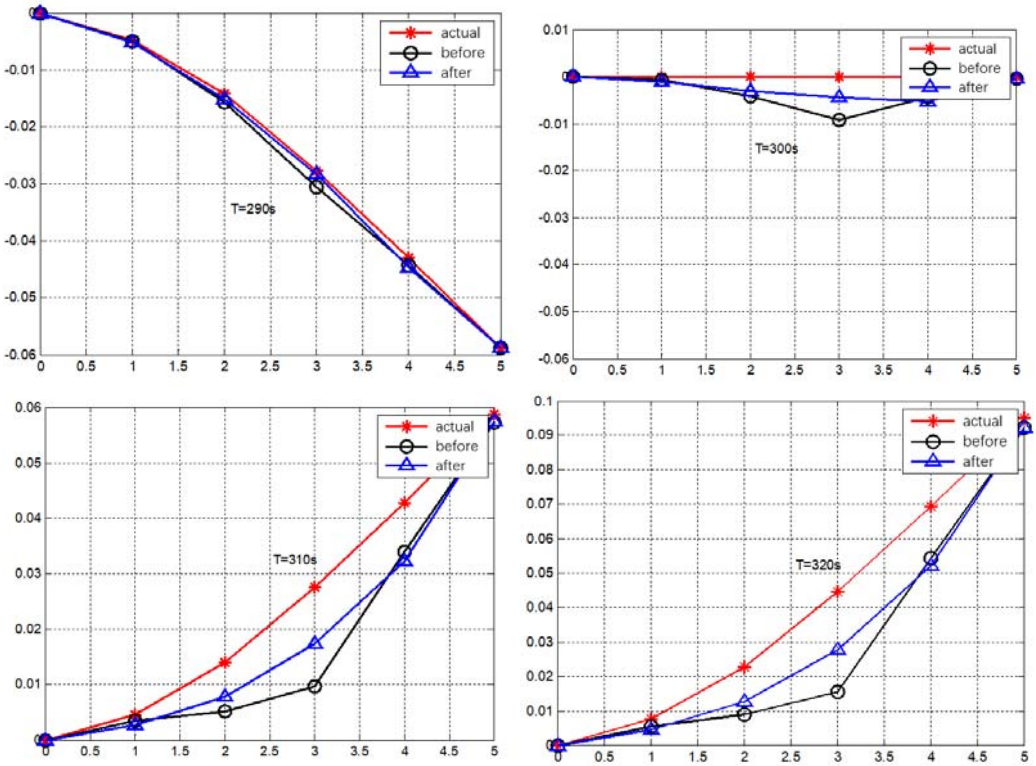

Figure 6 - Comparison of wing shape before and after fusion

It can be seen that after the relative position of each node is fused by the federated filter, the relative position error of the low-precision sub-nodes is significantly reduced, the relative position error of the medium-high-precision sub-nodes does not change much, and the shape of the wing is more Close to its actual value.

6. Conclusion

This paper proposes a new type of inertial network system based on MEMS inertial sensors, called distributed inertial reference system. The main research content includes the following aspects: (1) Relative navigation algorithm based on master and sub inertial navigation and its error Compensation method research; (2) Distributed inertial reference system fault tolerance method improvement and information fusion algorithm. The purpose is to provide high-precision inertial reference measurement information for local nodes even when the airframe produces flexural deformation and vibration in the air, and at the same time, it can monitor the deformation of the airframe. Theoretical and simulation results show that the real-time data of deformation and vibration can be measured locally under the condition of flexural deformation and vibration of the body.

References

[1] LU Y, CHENG X. Random misalignment and lever arm vector online estimation in shipborne aircraft transfer alignment[J]. Measurement, 2014,47: 756-764.

[2] Lu Y, Cheng X. Random misalignment and lever arm vector online estimation in shipborne aircraft transfer alignment[J]. Measurement, 2014, 47: 756-764.

[3] ALLERTON D J, JIA H. Distributed data fusion algorithms for inertial network systems[J]. IET Radar, Sonar & Navigation, 2008,2(1): 51-62.

[4] SHI W, LI X F, WANG C Y. Bending of a rectangular plate with rotationally restrained edges under a concentrated force[J]. Applied Mathematics and Computation, 2016,286: 265-278.

[5] Zhang Jing, Chen Hong-yue, Chen Yu, etc. A Multi-sensor Fusion Positioning Algorithm Based on Federate Kalman Filter[J]. MISSILES AND SPACE VEHICLES, 2018(02): 90-98.

[6] JIA H. Data fusion methodologies for multi sensor aircraft navigation systems[J]. 2004,58(3): 405-418.

[7] XING Z, XIA Y. Distributed Federated Kalman Filter Fusion Over Multi-Sensor Unreliable Networked Systems[J]. IEEE Transactions on Circuits & Systems I Regular Papers, 2016,63(10): 1-12.